Published in final edited form as:
Glia. 2014 December ; 62(12): 2022–2033. doi:10.1002/glia.22723.

Beneficial Effects of GFAP/Vimentin Reactive Astrocytes for Axonal Remodeling and Motor Behavioral Recovery in Mice after Stroke

Zhongwu Liu[1], **Yi Li**[1], **Yisheng Cui**[1], **Cynthia Roberts**[1], **Mei Lu**[2], **Ulrika Wilhelmsson**[3], **Milos Pekny**[3,4], and **Michael Chopp**[1,5]

[1]Department of Neurology, Henry Ford Hospital, Detroit, Michigan

[2]Department of Public Health Sciences, Henry Ford Health System, Henry Ford Health System, Detroit, Michigan

[3]Center for Brain Repair and Rehabilitation, Department of Clinical Neuroscience and Rehabilitation, Institute of Neuroscience and Physiology, Sahlgrenska Academy at University of Gothenburg, Gothenburg, Sweden

[4]Florey Institute of Neuroscience and Mental Health, Parkville, Victoria, Australia

[5]Department of Physics, Oakland University, Rochester, Michigan

Abstract

The functional role of reactive astrocytes after stroke is controversial. To elucidate whether reactive astrocytes contribute to neurological recovery, we compared behavioral outcome, axonal remodeling of the corticospinal tract (CST), and the spatio-temporal change of chondroitin sulfate proteoglycan (CSPG) expression between wild-type (WT) and glial fibrillary acidic protein/vimentin double knockout ($GFAP^{-/-}Vim^{-/-}$) mice subjected to Rose Bengal induced cerebral cortical photothrombotic stroke in the right forelimb motor area. A foot-fault test and a single pellet reaching test were performed prior to and on day 3 after stroke, and weekly thereafter to monitor functional deficit and recovery. Biotinylated dextran amine (BDA) was injected into the left motor cortex to anterogradely label the CST axons. Compared with WT mice, the motor functional recovery and BDA-positive CST axonal length in the denervated side of the cervical gray matter were significantly reduced in $GFAP^{-/-}Vim^{-/-}$ mice (n = 10/group, P <0.01). Immunohistological data showed that in $GFAP^{-/-}Vim^{-/-}$ mice, in which astrocytic reactivity is attenuated, CSPG expression was significantly increased in the lesion remote areas in both hemispheres, but decreased in the ischemic lesion boundary zone, compared with WT mice (n = 12/group, P <0.001). Our data suggest that attenuated astrocytic reactivity impairs or delays neurological recovery by reducing CST axonal remodeling in the denervated spinal cord. Thus, manipulation of astrocytic reactivity post stroke may represent a therapeutic target for neurorestorative strategies.

Address correspondence to Zhongwu Liu, Neurology Research, E&R Bldg., Room 3091, Henry Ford Hospital, 2799 West Grand Boulevard, Detroit, MI 48202, USA. zwliu@neuro.hfh.edu.

Keywords

reactive astrocytes; axonal remodeling; stroke recovery; glial scar

Introduction

Stroke is a leading cause of disability in adults worldwide. For decades, enormous efforts in experimental animal models of stroke have been devoted to the development of neuroprotective agents in an attempt to salvage ischemic neurons in the brain. However, all these efforts have failed to demonstrate efficacy in clinical trials of stroke (Rother, 2008), except for the administration of recombinant tissue plasminogen activator (tPA) within 4.5 h of stroke onset (Cronin, 2010).

Astrocytes are the most abundant subtypes of glial cells, and by several fold outnumber neurons in the central nervous system (CNS). Nevertheless, astrocytes have not been a major therapeutic target for the treatment of stroke, with most research emphasis on the neuron. As an integral part of the neuron–glia system, astrocytes provide many housekeeping functions, including structural support, neuronal metabolism, maintenance of the extracellular environment, regulation of cerebral blood flow, stabilization of cell–cell communications, neurotransmitter synthesis, and defense against oxidative stress (Ransom and Ransom, 2012). In the injured CNS, astrocytes undergo important morphological modifications, such as hyperplasia and hypertrophy, to form a glial scar, a physical and functional wall surrounding the damage area. These astrocytes, also referred to as, reactive Gliosis, exhibit increased expression of the intermediate filament proteins including glial fibrillary acidic protein (GFAP), vimentin, and nestin, and have altered expression of many other genes (Ridet et al., 1997).

The functional role of reactive astrocytes after stroke is controversial (Li et al., 2014). In the glial scar, reactive astrocytes express a broad range of inhibitory molecules against axonal regeneration, such as chondroitin sulfate proteoglycans (CSPGs) (McKeon et al., 1991). However, the glial scar may also seclude the injury site from healthy tissue, preventing a cascading wave of uncontrolled tissue damage (Faulkner et al., 2004). In addition, reactive astrocytes take up excess glutamate (Mazzanti et al., 2001), and produce neurotrophic factors (Hansson and Ronnback 2003), to protect the neurons from ischemic lesion. Thus, the reactivity of astrocytes after stroke may potentially play both detrimental and beneficial roles under certain spatiotemporal conditions.

In response to brain damage of stroke or trauma, reactive astrocytes upregulate GFAP and vimentin and reexpress nestin (Fuchs and Cleveland, 1998; Li and Chopp, 1999). In mice lacking both GFAP and vimentin ($GFAP^{-/-}Vim^{-/-}$), reactive gliosis and the glial scar are attenuated after neurotrauma (Pekny et al., 1999); however, at seventh day after induction of middle cerebral artery occlusion (MCAo), the infarct volume is 2.1–3.5 fold larger than in wild-type (WT) mice (Li et al., 2008). In addition, a recent *in vitro* study demonstrated that $GFAP^{-/-}Vim^{-/-}$ astrocytes exposed to oxygen–glucose deprivation and reperfusion exhibit increased cell death and confer lower degree of protection to cocultured neurons than WT astrocytes (de Pablo et al., 2013), suggesting that reactive astrocytes are protective during

brain ischemia. Considering the multifaceted effects of reactive astrocytes as inhibiting axonal growth and supporting neuronal survival, it is interesting to address the question of how reactive astrocytes affect neurological recovery post stroke? We, therefore, compared functional recovery, axonal remodeling of the corticospinal tract (CST), and the spatio temporal change of CSPG expression between WT and $GFAP^{-/-}Vim^{-/-}$ mice subjected to cerebral cortical photothrombotic stroke.

Materials and Methods

Animals

Breeder mice carrying a null mutation in the GFAP and vimentin genes ($GFAP^{-/-}Vim^{-/-}$) (Pekny et al., 1999) and the WT controls on a mixed genetic background of C57Bl/6–129Sv-129Ola were used. Adult (10–12 weeks old, body weight 22–27 g) male $GFAP^{-/-}Vim^{-/-}$ and age-matched WT mice used in this study were generated by our in-house breeding facility. A total of 44 animals (20 mice for behavioral and anatomical study, 24 mice for immunostaining) were used in this study. All experimental procedures were approved by the Institutional Animal Care and Use Committee of Henry Ford Hospital.

Surgical Procedure of Photothrombosis

To generate a consistent cerebral infarct volume in WT and $GFAP^{-/-}$ $Vim^{-/-}$ mice, focal cortical ischemia was induced by photothrombosis of the cortical microvessels with the photosensitive Rose Bengal technique, as previously described (Lee et al., 2007; Watson et al., 1985), with the following modifications. Briefly, under isoflurane anesthesia, the animal was restricted in a Kopf stereotaxic frame on a 37° C homeothermic blanket (Harvard Apparatus, Holliston, MA). Rose Bengal (100 μL, 10 mg/mL solution in saline; Sigma-Aldrich, St Louis, MO) was injected intraperitoneally 5 min before illumination. A midline incision of the scalp was performed to expose the skull. The skull was covered by a black plastic sheet with a hole to expose the area of 0.7–2.7 mm right to the midline, −1.0 to 2.5 mm rostral to the bregma, which included the caudal forelimb area and the rostral forelimb area (Jang et al., 2013). The brain was illuminated for 10 min through the exposed skull with a fiber-optic bundle of a cold light source (KL 1600 LED; Schott, Mainz, Germany) filtered with a green filter. Then the scalp was sutured and mice were allowed to awaken.

Behavioral Tests

Twenty mice subjected to photothrombosis were used for behavioral and anatomical studies (n = 10/group). To directly assess the voluntary motor deficits and recovery of the stroke-impaired left forepaw, a foot-fault test and a single pellet reaching test were performed before surgery, 3 days after stroke and weekly thereafter up to 4 weeks by an investigator blinded to the mouse phenotypes. The foot-fault test measures the accuracy of forepaw placement on a non-equidistant grid as the percentage of foot faults of the left forepaw to total steps (Hernandez and Schallert, 1988). The single pellet reaching test measures the ability of skilled forepaw use (Farr and Whishaw, 2002). The mice were placed in a Plexiglas box with a vertical slot on the front wall. Animals were trained for 5 days before surgery to use their left forepaw to extract 20 mg food pellets (Bio-Serv, Frenchtown, NJ) through the slot. A score of 1 was given when the animal was able to extract the pellet and

bring it to the mouth. If the animal dropped the pellet inside the box before eating, a score of 0.5 was given. If the mouse knocked the pellet off the shelf, a score of 0 was given. Performance of individual mouse was defined by the percentage of total score for reaching 20 pellets to the baseline score before stroke.

Anterograde CST Tracing

To validate the corticospinal axonal remodeling originating from the contralesional cortex, anterograde tracing was performed in the left intact cortex at 2 weeks after photothrombosis. Under isoflurane anesthesia, a unilateral craniotomy was performed over the left frontal motor cortex with a high speed drill (Foredom Electric, Bethel, CT). Ten percent solution of biotinylated dextran amine (BDA, 10,000 MW; Molecular Probes, Eugene, OR) in saline was injected into four points in the left frontal motor cortex using a finely drawn glass capillary injector (100 nL per injection; stereotaxic coordinates: 0 and 0.5 mm rostral to the bregma, 1.5 and 2.0 mm lateral to the midline; 0.7 mm deep to the dura) (Paxinos and Franklin, 1997). The micropipette remained in place for 4 min after completion of the injection.

Tissue Preparation and CST Axonal Measurement

Animals were allowed to survive for 4 weeks after photothrombosis. Under deep Ketamine anesthesia, the mice were perfused transcardialy with saline, followed by 4% paraformaldehyde. The entire brain and spinal cord were immersed in 4% paraformaldehyde overnight. The brain was cut into seven equally spaced (1 mm) coronal blocks. The brain blocks and the cervical spinal tissues were embedded in paraffin. A series of adjacent 6-μm thick sections were cut from each block and stained with Hematoxylin and Eosin for lesion volume evaluation measured as percentage of the lesion area compared with the contralateral hemisphere, as previously described (Swanson et al., 1990). The cervical spinal tissues were processed for 100-μm thick traverse sections using a vibratome. The spinal sections were incubated with avidin–biotin–peroxidase complex (Vector Laboratories, Burlingame, CA) at 4°C for 48 h, and the BDA-labeling was visualized with 3,3'-diaminobenzidine (DAB)-nickel (Vector).

The length of BDA-positive CST axons in the stroke-impaired side of the ventral gray matter was measured on 30 consecutive transverse sections of the cervical cord (C5–7) for each animal using a plug-in NeuroJ in the NIH image software (ImageJ). The number of BDA-positive fibers in the pyramidal tract at the medulla level ipsilateral to the injection site were counted and averaged on three consecutive coronal sections for each animal. To avoid inter-animal variation in tracing efficiency, CST remodeling was estimated by the total BDA-labeled axonal length normalized with a quotient of individual BDA-labeled CST number in the pyramidal tract to the average number calculated in all animal groups.

Immunohistochemistry

Separate animal groups of normal and stroke mice euthanatized on days 3, 7, and 14 after photothrombosis (n = 3/time point) were used for immunostaining. Following deparaffinization, 6-μm thick paraffin coronal brain and spinal sections obtained from WT and GFAP$^{-/-}$ Vim$^{-/-}$ mice were processed for either single label (visualized with DAB) or

double label (visualized with FITC and CY3) immunostaining using standard procedures. Primary antibodies against GFAP (Dako, Carpinteria, CA), vimentin (Abcam, Cambridge, MA), nestin (BD biosciences, Franklin Lakes, NJ), S100beta (Dako), CSPG (CS-56, LifeSpan Biosciences, Seattle, WA), NeuN (Millipore, Billerica, MA), APC (GenWay Biotech, San Diego, CA), and IBa1 (Wako, Richmond, VA) were used. ImageJ was used for quantitative measurements of DAB precipitates shown as percentage of relative proportional areas.

Statistics

The mixed model, analysis variance and covariance (ANCOVA), was performed to analyze the differences in behavioral outcome between WT and GFAP$^{-/-}$ Vim$^{-/-}$ mice before and after stroke. Two- sample *t*-test was used to test the significance in lesion volume, BDA-labeled axonal length, and CSPG positive immunostaining areas between two groups. All data are presented as mean ± SD. A value of $P < 0.05$ was taken as significant.

Results

Infarct Volume and Behavioral Outcome after Cortical Photothrombotic Stroke

In order to investigate the effect of reactive astrocytes on neurological recovery after stroke, we compared the behavioral outcome during the recovery process between WT mice and GFAP$^{-/-}$Vim$^{-/-}$ mice. For this purpose, we performed Rose Bengal induced photothrombosis to the forelimb motor cortex. As shown in Fig. 1A, the ischemic infarct was localized to the directly illuminated cortical tissue. Unlike increased infarct volume observed in GFAP$^{-/-}$Vim$^{-/-}$ mice compared with that in WT mice 7 days after distal middle cerebral artery transection in a previous study (Li et al., 2008), there was no significant difference in the lesion volume between WT and GFAP$^{-/-}$Vim$^{-/-}$ mice 28 days after cortical photothrombosis (1B). In addition, the modest cortical lesion in the right fore-limb area led to severe, however, comparable behavioral deficits of the left forepaw in both WT and GFAP$^{-/-}$Vim$^{-/-}$ mice starting 3 days after stroke measured with foot-fault test (Fig. 2A) and single pellet reaching test (Fig. 2B). Gradual recovery was observed in both WT and GFAP$^{-/-}$Vim$^{-/-}$ mice; however, compared with WT mice, the motor performance of the left forepaw in GFAP$^{-/-}$Vim$^{-/-}$ mice was significantly reduced from day 14 to day 28 after stroke.

Contralesional CST Axonal Plasticity Impaired in GFAP$^{-/-}$Vim$^{-/-}$ Mice after Stroke

Based on our prior findings that unilateral cerebral stroke induces contralesional midline-crossing remodeling of the CST axons in the spinal cord (Liu et al., 2008), contributing to behavioral recovery after stroke (Liu et al., 2013), we further investigated contralesional CST axonal plasticity by injecting BDA into the forelimb area of the contralesional cortex, to anterogradely label the CST axons (Fig. 3A). In WT mice subjected to unilateral right photothrombosis in the forelimb cortical area, in the denervated left side of the cervical cord, BDA-labeled contralesional CST axons that crossed the midline of the spinal cord, and extended toward the ventral horn (Fig. 3B), were evident, while in GFAP$^{-/-}$Vim$^{-/-}$ mice, BDA-labeled CST axons were rarely observed in the left denervated spinal cord (Fig. 3C). We measure the BDA-labeled axonal length on 30 consecutive cervical sections in each

animal. Quantitative data showed that the total length of BDA-labeled CST axons was significantly reduced in GFAP$^{-/-}$Vim$^{-/-}$ mice (Fig. 3D, P<0.001).

CSPG Expression is Increased in GFAP$^{-/-}$Vim$^{-/-}$ Mice with Attenuated Astrocytic Reactivity after Stroke

To identify astrocytic reactivity after induction of the ischemic lesion, we performed immunostaining using antibodies against astrocytic markers of GFAP, vimentin, nestin, and S100β in WT and GFAP$^{-/-}$Vim$^{-/-}$ mouse brains (Fig. 4). Three days after stroke, hypertrophic astrocytes were detected with GFAP (Fig. 4B) and vimentin (Fig. 4E) immunostaining in the cortical area surrounding the lesion in WT mice, but not in GFAP$^{-/-}$Vim$^{-/-}$ mice (Fig. 4C,F). Since nestin is expressed in developing astrocytes and absent in mature astrocytes, and re-expressed after injury, nestin was used as a marker of reactive astrocytes (Li and Chopp, 1999). Nestin expression was found in the vicinity of the lesion in both WT and GFAP$^{-/-}$Vim$^{-/-}$ mice after stroke (Fig. 4G – I). However, the expression of nestin was strong and continuous in WT mice, but weak and transient only for 3 days, and then barely detected in GFAP$^{-/-}$Vim$^{-/-}$ mice, consistent with our previous data from needle injury of the brain cortex (Eliasson et al., 1999). S100β is a marker of mature astrocytes (Cocchia, 1981). We performed double immunofluorescent staining for S100β and GFAP or nestin in WT mice. S100β expression was found in the cell body and thick processes of most GFAP (Fig. 4J) or nestin (Fig. 4K) positive astrocytes. Therefore, S100β antibody was used to identify astrocytes in GFAP$^{-/-}$Vim$^{-/-}$ mice. S100β positive astrocytes were detected in GFAP$^{-/-}$Vim$^{-/-}$ mouse brain (Fig. 4L), and the expression level of S100β was comparable before and after stroke in both WT and GFAP$^{-/-}$Vim$^{-/-}$ mice (data not shown).

Reactive astrocyte generated CSPGs are the major inhibitory components of neurite outgrowth in glial scarring following CNS injury (McKeon et al., 1991). To investigate whether reduced CST axonal plasticity in GFAP$^{-/-}$Vim$^{-/-}$ mice is associated with CSPG, we examined the distribution of CSPG in both ipsilesional and contralesional cerebral hemispheres with immunohistochemistry using monoclonal CSPG antibody CS56, which is specific for the glycosaminoglycan (GAG) portion of native CSPG with epitope recognizing CS octasaccharide containing A–D tetrasaccharide sequence (Deepa et al., 2007; Ito et al., 2005). The CSPG positive staining in GFAP$^{-/-}$Vim$^{-/-}$ mice showed a distinct patchy pattern, referred to in a study on the WT mouse cortex as, dandelion clock-like structure (Hayashi et al., 2007). In the present study, we found this pattern was also present in the corpus callosum and striatum of GFAP$^{-/-}$Vim$^{-/-}$ mice (Fig. 5). In the contralesional cerebral hemisphere, CSPG expression increased as early as day 3 after stroke in both WT (Fig. 5A – D) and GFAP$^{-/-}$Vim$^{-/-}$ mice (Fig. 5E – H), while at day 14 after stroke, CSPG in the contralateral hemisphere decreased in WT mice, but further increased in GFAP$^{-/-}$Vim$^{-/-}$ mice. Quantitative data showed that CSPG expression in the contralesional hemisphere at day 14 after stroke was significantly higher in GFAP$^{-/-}$Vim$^{-/-}$ mice than in WT mice (Fig. 5L). Interestingly, in the ipsilesional hemisphere, increased CSPG expression was observed in the ischemic lesion boundary zone (arrows) in WT mice (Fig. 5I – K); however, in GFAP$^{-/-}$Vim$^{-/-}$ mice, CSPG expression was increased in the cortical area outer lesion boundary zone (arrowheads), but not in the lesion boundary zone (Fig. 5M – O).

Quantitative measurements of CSPG positive areas in the ischemic lesion boundary zone and the cortical area outer lesion boundary zone showed significant differences between WT and GFAP$^{-/-}$Vim$^{-/-}$ mice (Fig. 5P).

To reveal the potential cellular sources and targets of CSPG, we performed double immunostaining with antibodies against CSPG and S100β, NeuN, APC, NG2, or IBa1to characterize astrocytes, neurons, oligodendrocytes, oligodendrocyte precursor cells, and microglial cells, respectively (Fig. 6). We found that a subpopulation, but not all astrocytes (Fig. 6A – C) and neurons (Fig. 6D – F) were surrounded by CSPG, while oligodendrocytes (Fig. 6G – I), immature oligodendrocytes (Fig. 6J – L), and microglial cells (Fig. 6M – O) were distant from CSPG, consistent with the results from Wakada et al. (Hayashi et al., 2007).

Discussion

In this study, we examined whether the absence of the two major astrocytic intermediate filament proteins, GFAP and Vimentin, would impact functional recovery and axonal remodeling after stroke, since reactive astrocytes purportedly act as a barrier, inhibiting neuronal regeneration and neurite outgrowth (Silver and Miller, 2004). We, therefore, investigated functional recovery and axonal remodeling in GFAP$^{-/-}$Vim$^{-/-}$ mice, which are devoid of astrocytic intermediate filaments and show attenuated reactive gliosis and scar formation after CNS injury (Pekny et al., 1999). The astrocytic nanofilament system is a structural component of the cytoskeleton and serves as an important signaling platform in situations linked to cellular stress (Hyder et al., 2011; Pallari and Eriksson, 2006; Pekny and Lane, 2007). In injured brains of GFAP$^{-/-}$Vim$^{-/-}$ mice, astrocytes show similar abundance and access comparable volumes of brain tissue as astrocytes of wild-type mice (Wilhelmsson et al., 2004), but do not exhibit the reactive phenotype with characteristic hypertrophic processes as astrocytes in wild-type mice (Li et al., 2008; Wilhelmsson et al., 2004, 2006). Glial scar formation is attenuated in GFAP$^{-/-}$Vim$^{-/-}$ mice, healing after trauma takes longer and post-traumatic synaptic loss is more prominent (Pekny et al., 1999; Wilhelmsson et al., 2004). The astrocyte intermediate filament system influences viscoelastic properties of astrocytes (Lu et al., 2011), intracellular vesicle trafficking (Potokar et al., 2007, 2010; Vardjan et al., 2012), and is important for astrocyte response to hypoosmotic stress (Ding et al., 1998), spontaneous astrocyte motility (Lepekhin et al., 2001), and highly probably also for the interaction of astroglial cells with microglia or blood borne monocytes (Kraft et al., 2013; Macauley et al., 2011; Nakazawa et al., 2007). Genetic ablation of GFAP and vimentin when combined with neuronal overexpression of Bcl-2 improves regeneration of the severed optic nerve in the postnatal period (Cho et al. 2005). Regenerative responses and functional recovery after spinal cord trauma is improved in GFAP$^{-/-}$Vim$^{-/-}$ mice (Menet et al., 2003), which also show increased hippocampal neurogenesis in adulthood (Wilhelmsson et al., 2012), and in older mice (Larsson et al., 2004). GFAP$^{-/-}$Vim$^{-/-}$ mice support better integration of neural grafts (Kinouchi et al., 2003) and increased neuronal and astrocytic differentiation from neural stem cells transplanted in the hippocampus (Widestrand et al., 2007). Thus, at least in some disease contexts, the benefits of reactive gliosis at the acute injury phase seem to be counteracted by restricted regenerative potential at later stages (Pekny et al., 2014). Surprisingly, in the

present study compared with WT mice, GFAP$^{-/-}$Vim$^{-/-}$ mice subjected to cortical ischemia exhibited attenuated astrocytic reactivity, significantly reduced or delayed motor functional recovery and CST axonal remodeling, associated with a distinctive CSPG distribution. In contrast with WT mice, CSPG was significantly increased in the contralesional cerebral hemisphere and in the cortical area of the outer ischemic lesion boundary zone in the ipsilesional hemisphere of GFAP$^{-/-}$Vim$^{-/-}$ mice. The reduced functional recovery and CST plasticity observed in GFAP$^{-/-}$Vim$^{-/-}$ mice after stroke compared with WT mice, may in-part be attributed to the increased CSPG expression in the contralateral and remote ipsilateral hemispheres in GFAP$^{-/-}$Vim$^{-/-}$ mice.

Because of the overlap between the MCA and anterior cerebral artery (ACA) territories, there is a relatively wide blood flow transition zone (from fully flowing to severely depressed) in the area of MCA territory during MCAo (Li and Murphy, 2008). A recent study demonstrated that astrocytes derived from GFAP$^{-/-}$Vim$^{-/-}$ mice exposed to oxygen-glucose deprivation and reperfusion exhibited increased cell death, and conferred a lower degree of protection compared with cocultured neurons than WT astrocytes (de Pablo et al., 2013). Also, the ischemic stroke penumbra may be more compromised in GFAP$^{-/-}$Vim$^{-/-}$ mice because of reduced glutamate transport, less effective endothelin 3-induced blockage of gap-junctional communication between GFAP$^{-/-}$Vim$^{-/-}$ astrocytes potentially allowing expansion of the ischemic lesion over time, and lower levels of PAI-1 that may lead to a decreased protection against tPA-induced neurotoxicity (Li et al., 2008). Thus, MCA transection induces larger infarct volume in GFAP$^{-/-}$Vim$^{-/-}$ mice than in WT mice (Li et al., 2008), which may lead to incomparable functional outcome during the recovery phase after stroke. The photosensitive dye (Rose Bengal) becomes activated and induces endothelial damage with platelet activation and thrombosis, when illuminated by a cold light source, resulting in local blood flow interruption by a rapidly evolving ischemic damage without salvageable penumbra (Lee et al., 2007; Watson et al., 1985). Therefore, to avoid the variation in lesion volume on behavioral recovery after stroke, we performed a unilateral photothrombosis to the forelimb motor area to generate a consistent focal cortical ischemia of equivalent size in both WT and GFAP$^{-/-}$Vim$^{-/-}$ mice. In addition, since the light source can be applied to target any cortical area of interest determined by the size of the illuminated area, this technique is highly advantageous for precise functional studies.

The present study employed two behavioral tests, the footfault test and single pellet reaching test, to estimate the neurological outcome of the left forepaw in mice subjected to right forelimb motor area lesion. In both behavioral tests used in this study, the mice need to voluntarily control the paw movement through the corticospinal innervations. Our observations of reduced behavioral recovery and CST axonal remodeling in GFAP$^{-/-}$Vim$^{-/-}$ mice indicated a substantial contribution of astrocytic reactivity to neurological recovery after CNS lesion. Consistent with previous studies (Menet et al., 2003; Pekny et al., 1999; Wilhelmsson et al., 2004), our results indicated that mice deficient in both GFAP and vimentin genes exhibit attenuated astrocytic reactivity after cortical stroke. In WT mice, this reactivity was demonstrated by upregulated expression of GFAP, vimentin and nestin, while in mice with absence of GFAP and vimentin, nestin, the marker of reactive astrocytes, was only transiently increased after stroke. The weak and transient nestin immunoreactivity in GFAP$^{-/-}$Vim$^{-/-}$ astrocytes in the cerebral cortex surrounding the lesion is conceivably a

consequence of the absence of vimentin, a polymerization partner of nestin, resulting in decreased nestin protein levels in $GFAP^{-/-}Vim^{-/-}$ astrocytes (Eliasson et al., 1999). Neural stem/progenitor cells have been identified in the subventricular and subgranular zones of the hippocampus (Lagace et al., 2007), as well as the cerebral cortex after stroke (Nakagomi et al., 2009). Since nestin is also a neural stem/progenitor cell marker (Morshead et al., 1994), further studies are needed to examine the potential effect of reactive astrocytes on endogenous neurogenesis after stroke. $GFAP^{-/-}Vim^{-/-}$ mice exhibited a reduced scar formation in the lesion boundary region, detected with immunostaining of CSPG, the major barrier component in the glial scar. Unexpectedly, our behavioral functional data showed that the attenuated glial scar did not lead to improved functional recovery after stroke, as in the increased functional restoration observed in $GFAP^{-/-}Vim^{-/-}$ mice subjected to spinal cord injury (Menet et al., 2003). This indicated that unlike spinal cord injury, the glial scar formation in the infarct proximal boundary region may not be a major barrier factor for neurological recovery after cerebral stroke. After spinal cord injury, extension of axons to bridge damage, may enhance functional recovery. Thus, reduced scar formation and reduced CSPG at the site of the damage may foster neurite growth and functional recovery. In contrast, after induction of stroke, reduction of the adjacent glial scar and reduction of CSPG, likely has no beneficial effect, since there is no neural cell survival in the ischemic infarct core area, thus, no necessity or benefit of promoting neurite extension and growth crossing the glial scar into the lesion boundary zone. To the contrary, our data suggest that the glial scar may have restorative effects, and restricts the ischemic lesion, and thereby promotes neurological recovery post stroke. As previously noted, absence of GFAP and vimentin improved post-traumatic synaptic regeneration in the hippocampus in mice, however, behavioral data were not reported (Wilhelmsson et al., 2004). We cannot exclude the possibility, that photothrombotic stroke leads to a delayed, rather than reduced, CSTaxonal remodeling and neurological recovery in mice deficient for GFAP and vimentin, since 4 weeks post stroke these mice continued to improve their motor functions. In support of this premise, we recently reported delayed but complete axonal regeneration after sciatic nerve lesion in $GFAP^{-/-}Vim^{-/-}$ mice that implied altered response dynamics but a comparable outcome after peripheral nervous system lesion in mice deficient in the intermediate filament system in astrocytes and Schwann cells (Berg et al., 2013).

Studies in both animals and humans show that the adult mammalian brain has potential to drive structural and functional reorganization mediating recovery after stroke (Dancause, 2006; Nudo, 2006). Unilateral stroke in the primary motor cortex leads to functional compensation in the contralesional hemisphere in patients with greater recovery (Biernaskie et al., 2005; Johansen-Berg et al., 2002; Strens et al., 2003). In rodents subjected to unilateral MCAo, CST axons originating from the contralesional cortex re-cross the midline of the spinal cord into the denervated gray matter (Liu et al,. 2007), and this axonal remodeling contributes to motor recovery (Liu et al., 2011). Growth factors promote lesionremote plasticity of the contralesional pyramidal tract, but do not further increase axonal sprouting in the injured hemisphere (Reitmeir et al., 2012). To investigate the neuroanatomical substrate of the behavioral recovery in mice subjected to photothrombosis in the right side of the forelimb motor cortex, we labeled the CST axons originating from the contralesional forelimb motor area with intracortical injection of anterograde neuronal

tracer, BDA. Our results showed that contralesional axonal remodeling was significantly reduced in GFAP$^{-/-}$Vim$^{-/-}$ mice compared with WT mice.

Astrocytic glial scar formation isolates the injury site to protect spared tissue from further damage (Bush et al., 1999). Reactive astrocytes restrict the lesion and minimize the area of inflammation in the acute stage after CNS injury (Sofroniew, 2005), and may also restrict diffusible factors secreted from the lesion region into remote area. Thus, our observation of increased CSPG expression in the cortical area outer ischemic lesion boundary zone and the contralesional cerebral hemisphere in GFAP$^{-/-}$Vim$^{-/-}$ mice may be attributed to the attenuated glial scar formation in the lesion boundary zone. CSPGs are a family of molecules including aggrecan, brevican, neurocan, versican, phosphacan, and NG2, characterized by a protein core to which large, highly sulphated GAG chains are attached (Morgenstern et al., 2002). After injury, CSPG expression is rapidly upregulated by reactive astrocytes, forming an inhibitory gradient that is highest at the centre of the lesion and diminishes gradually into the penumbra (McKeon et al., 1991). The inhibitory activity of CSPGs depends on the GAG components, as treatment with chondroitinase ABC, an enzyme that removes GAG chains from the protein core, eliminates this inhibition (Silver and Miller, 2004). The expression of CSPG characterized by the CS-56 antibody, which recognizes the CS GAG region, was previously identified in a subpopulation of astrocytes (Hayashi et al., 2007). Our results of increased CSPG expression in the areas remote from the lesion including the contralesional cerebral hemisphere and the cortical area outer lesion boundary zone in the ipsilesional hemisphere in GFAP$^{-/-}$Vim$^{-/-}$ mice, suggest that subpopulations of astrocytes lacking GFAP and vimentin respond to injury to upregulate CSPG expression. Thus, the reduced CST axonal remodeling and neurological recovery in GFAP$^{-/-}$Vim$^{-/-}$ mice after stroke may be attributed to upregulated CSPG expression in the remote areas surrounding a subpopulation of astrocytes and neurons, although the specific types of these astrocytes and neurons remain to be further characterized. Our findings that reduced CSPG distribution in the lesion boundary zone in GFAP$^{-/-}$Vim$^{-/-}$ mice was accompanied with impaired functional recovery, further indicated that the glial scar provides beneficial effects to neurological recovery after cortical stroke, consistent with our previous study that the functional recovery after stroke is associated to distal local axonal sprouting and outgrowth within the denervated spinal gray matter, rather than long distance axonal regeneration originating from the brain (Liu et al., 2008).

Neurite extension may depend on a balance of growth-promoting and growth-inhibiting molecules in the extracellular matrix after injury. The CNS response to stroke is a multicellular process that changes continually over time and is regulated by a multitude of extracellular and intracellular molecular signaling events (Burda and Sofroniew, 2014). Depending on the timing and local environments after stroke, reactive astrocytes may be beneficial or detrimental (Lo, 2008). In the setting of ischemia, attenuation of reactive gliosis by genetic ablation of GFAP and vimentin leads to increased infarction (Li et al., 2008) and synapse loss (Wilhelmsson et al., 2004), suggesting that reactive astrocytes play an important role in the protection of the ischemic penumbra. Recent work also suggests that astrocytes promote neurorestoration several days to weeks after injury (Zhao and Rempe, 2010). Astrocytes, together with microglia, also release trophic factors such as basic fibroblast growth factor, nerve growth factor, ciliary neurotrophic factor (Hansson and

Ronnback, 2003), glial cell line-derived growth factor (Schaar et al., 1993), and brain-derived neurotrophic factor (Bejot et al., 2011), thus promoting neuronal plasticity, synaptic formation, and rebuilding of the nervous system to improve functional outcome after injury (Privat, 2003; Trendelenburg and Dirnagl, 2005). In contrast, reactive astrocytes may release proteolytic molecules, such as matrix metalloproteinases (Hsu et al., 2006), to degrade CSPGs (Zuo et al., 1998), as observed in the present study that attenuated astrocytic activation induced increased CSPG expression in $GFAP^{-/-}Vim^{-/-}$ mice. Several forms of astrocytes exist in the CNS, including fibrous (in white matter), protoplasmic (in grey matter), and radial (Marin-Padilla, 1995; Shannon et al., 2007). For isomorphic reactive astrocytes, the balance is inhibitory for central neurite outgrowth, while anisomorphic reactive astrocytes probably express inhibitory components at lower levels and the growth promoting factors predominate (Bovolenta et al., 1991). In the present study, the CSPG expression was distributed to a subpopulation of astrocytes, suggesting that a different subtype of astrocytes may respond to the lesion differently. Further investigation is needed to reveal what kind of astrocytes and how they provide beneficial or detrimental effects to stroke recovery.

Although reactive astrocytes form an inhibitory glial scar following stroke, they also perform functions important in neural repair. Our findings suggest that the involvement of astrocytes in axonal remodeling and functional recovery after stroke may represent a possible therapeutic target for neurorestorative strategies. Further studies focused on preserving reactive astrocytes, to augment their protective functions, and/or reduce their detrimental effects, may lead to novel approaches to improve neurological recovery after stroke.

Acknowledgment

Grant sponsor: National Institute of Neurological Disorders and Stroke (NINDS) of the National Institutes of Health; Grant number: R01AG037506 (MC) and R01NS066041 (ZL); Grant sponsor: EU FP 7 Program *TargetBraIn*; Grant number: 279017.

The authors thank Ms. Qing-e Lu and Ms. Yan Wang for their technical assistances, and Prof. Jin-Moo Lee (Washington University School of Medicine) for his kind help with establishing the colony of $GFAP^{-/-}Vim^{-/-}$ mice.

References

Bejot Y, Prigent-Tessier A, Cachia C, Giroud M, Mossiat C, Bertrand N, Garnier P, Marie C. Time-dependent contribution of non neuronal cells to BDNF production after ischemic stroke in rats. Neurochem Int. 2011; 58:102–111. [PubMed: 21074587]

Berg A, Zelano J, Pekna M, Wilhelmsson U, Pekny M, Cullheim S. Axo-nal regeneration after sciatic nerve lesion is delayed but complete in GFAP-and vimentin-deficient mice. PLoS One. 2013; 8:e79395. [PubMed: 24223940]

Biernaskie J, Szymanska A, Windle V, Corbett D. Bi-hemispheric contribution to functional motor recovery of the affected forelimb following focal ischemic brain injury in rats. Eur J Neurosci. 2005; 21:989–999. [PubMed: 15787705]

Bovolenta P, Wandosell F, Nieto-Sampedro M. Neurite outgrowth over resting and reactive astrocytes. Restor Neurol Neurosci. 1991; 2:221–228. [PubMed: 21551606]

Burda JE, Sofroniew MV. Reactive gliosis and the multicellular response to CNS damage and disease. Neuron. 2014; 81:229–248. [PubMed: 24462092]

Bush TG, Puvanachandra N, Horner CH, Polito A, Ostenfeld T, Svendsen CN, Mucke L, Johnson MH, Sofroniew MV. Leukocyte infiltration, neuronal degeneration, and neurite outgrowth after ablation of scar-forming, reactive astrocytes in adult transgenic mice. Neuron. 1999; 23:297–308. [PubMed: 10399936]

Cho KS, Yang L, Lu B, Feng Ma H, Huang X, Pekny M, Chen DF. Reestablishing the regenerative potential of central nervous system axons in postnatal mice. J Cell Sci. 2005; 118:863–872. [PubMed: 15731004]

Cocchia D. Immunocytochemical localization of S-100 protein in the brain of adult rat. An ultrastructural study. Cell Tissue Res. 1981; 214:529–540. [PubMed: 7214465]

Cronin CA. Intravenous tissue plasminogen activator for stroke: A review of the ECASS III results in relation to prior clinical trials. J Emerg Med. 2010; 38:99–105. [PubMed: 19765940]

Dancause N. Vicarious function of remote cortex following stroke: Recent evidence from human and animal studies. Neuroscientist. 2006; 12:489–499. [PubMed: 17079515]

de Pablo Y, Nilsson M, Pekna M, Pekny M. Intermediate filaments are important for astrocyte response to oxidative stress induced by oxygen-glucose deprivation and reperfusion. Histochem Cell Biol. 2013; 140:81–91. [PubMed: 23756782]

Deepa SS, Yamada S, Fukui S, Sugahara K. Structural determination of novel sulfated octasaccharides isolated from chondroitin sulfate of shark cartilage and their application for characterizing monoclonal antibody epitopes. Glycobiology. 2007; 17:631–645. [PubMed: 17317718]

Ding M, Eliasson C, Betsholtz C, Hamberger A, Pekny M. Altered tau-rine release following hypotonic stress in astrocytes from mice deficient for GFAP and vimentin. Brain Res Mol Brain Res. 1998; 62:77–81. [PubMed: 9795147]

Eliasson C, Sahlgren C, Berthold CH, Stakeberg J, Celis JE, Betsholtz C, Eriksson JE, Pekny M. Intermediate filament protein partnership in astrocytes. J Biol Chem. 1999; 274:23996–24006. [PubMed: 10446168]

Farr TD, Whishaw IQ. Quantitative and qualitative impairments in skilled reaching in the mouse (Mus musculus) after a focal motor cortex stroke. Stroke. 2002; 33:1869–1875. [PubMed: 12105368]

Faulkner JR, Herrmann JE, Woo MJ, Tansey KE, Doan NB, Sofroniew MV. Reactive astrocytes protect tissue and preserve function after spinal cord injury. J Neurosci. 2004; 24:2143–2155. [PubMed: 14999065]

Fuchs E, Cleveland DW. A structural scaffolding of intermediate filaments in health and disease. Science. 1998; 279:514–519. [PubMed: 9438837]

Hansson E, Ronnback L. Glial neuronal signaling in the central nervous system. FASEB J. 2003; 17:341–348. [PubMed: 12631574]

Hayashi N, Tatsumi K, Okuda H, Yoshikawa M, Ishizaka S, Miyata S, Manabe T, Wanaka A. DACS, novel matrix structure composed of chondroitin sulfate proteoglycan in the brain. Biochem Biophys Res Commun. 2007; 364:410–415. [PubMed: 17950248]

Hernandez TD, Schallert T. Seizures and recovery from experimental brain damage. Exp Neurol. 1988; 102:318–324. [PubMed: 3197789]

Hsu JY, McKeon R, Goussev S, Werb Z, Lee JU, Trivedi A, Noble-Haeusslein LJ. Matrix metalloproteinase-2 facilitates wound healing events that promote functional recovery after spinal cord injury. J Neurosci. 2006; 26:9841–9850. [PubMed: 17005848]

Hyder CL, Isoniemi KO, Torvaldson ES, Eriksson JE. Insights into intermediate filament regulation from development to ageing. J Cell Sci. 2011; 124:1363–1372. [PubMed: 21502133]

Ito Y, Hikino M, Yajima Y, Mikami T, Sirko S, von Holst A, Faissner A, Fukui S, Sugahara K. Structural characterization of the epitopes of the monoclonal antibodies 473HD, CS-56, and MO-225 specific for chondroitin sulfate D-type using the oligosaccharide library. Glycobiology. 2005; 15:593–603. [PubMed: 15625183]

Jang SH, Chang CH, Lee J, Kim CS, Seo JP, Yeo SS. Functional role of the corticoreticular pathway in chronic stroke patients. Stroke. 2013; 44:1099–1104. [PubMed: 23444306]

Johansen-Berg H, Rushworth MF, Bogdanovic MD, Kischka U, Wimalaratna S, Matthews PM. The role of ipsilateral premotor cortex in hand movement after stroke. Proc Natl Acad Sci U S A. 2002; 99:14518–14523. [PubMed: 12376621]

Kinouchi R, Takeda M, Yang L, Wilhelmsson U, Lundkvist A, Pekny M, Chen DF. Robust neural integration from retinal transplants in mice deficient in GFAP and vimentin. Nat Neurosci. 2003; 6:863–868. [PubMed: 12845328]

Kraft AW, Hu X, Yoon H, Yan P, Xiao Q, Wang Y, Gil SC, Brown J, Wilhelmsson U, Restivo JL, Cirrito JR, Holtzman DM, Kim J, Pekny M, Lee JM. Attenuating astrocyte activation accelerates plaque pathogenesis in APP/PS1 mice. FASEB J. 2013; 27:187–198. [PubMed: 23038755]

Lagace DC, Whitman MC, Noonan MA, Ables JL, DeCarolis NA, Arguello AA, Donovan MH, Fischer SJ, Farnbauch LA, Beech RD. Dynamic contribution of nestin-expressing stem cells to adult neurogenesis. J Neurosci. 2007; 27:12623–12629. others. [PubMed: 18003841]

Larsson A, Wilhelmsson U, Pekna M, Pekny M. Increased cell proliferation and neurogenesis in the hippocampal dentate gyrus of old $GFAP^{-/-}Vim^{-/-}$ mice. Neurochem Res. 2004; 29:2069–2073. [PubMed: 15662841]

Lee JK, Park MS, Kim YS, Moon KS, Joo SP, Kim TS, Kim JH, Kim SH. Photochemically induced cerebral ischemia in a mouse model. Surg Neurol. 2007; 67:620–625. [PubMed: 17512331]

Lepekhin EA, Eliasson C, Berthold CH, Berezin V, Bock E, Pekny M. Intermediate filaments regulate astrocyte motility. J Neurochem. 2001; 79:617–625. [PubMed: 11701765]

Li L, Lundkvist A, Andersson D, Wilhelmsson U, Nagai N, Pardo AC, Nodin C, Stahlberg A, Aprico K, Larsson K. Protective role of reactive astrocytes in brain ischemia. J Cereb Blood Flow Metab. 2008; 28:468–481. others. [PubMed: 17726492]

Li P, Murphy TH. Two-photon imaging during prolonged middle cerebral artery occlusion in mice reveals recovery of dendritic structure after reperfusion. J Neurosci. 2008; 28:11970–11979. [PubMed: 19005062]

Li Y, Chopp M. Temporal profile of nestin expression after focal cerebral ischemia in adult rat. Brain Res. 1999; 838:1–10. [PubMed: 10446310]

Li Y, Liu Z, Xin H, Chopp M. The role of astrocytes in mediating exogenous cell-based restorative therapy for stroke. Glia. 2014; 62:1–16. [PubMed: 24272702]

Liu Z, Chopp M, Ding X, Cui Y, Li Y. Axonal remodeling of the corticospinal tract in the spinal cord contributes to voluntary motor recovery after stroke in adult mice. Stroke. 2013; 44:1951–1956. [PubMed: 23696550]

Liu Z, Li Y, Qu R, Shen L, Gao Q, Zhang X, Lu M, Savant-Bhonsale S, Borneman J, Chopp M. Axonal sprouting into the denervated spinal cord and synaptic and postsynaptic protein expression in the spinal cord after transplantation of bone marrow stromal cell in stroke rats. Brain Res. 2007; 1149:172–180. [PubMed: 17362881]

Liu Z, Li Y, Zhang RL, Cui Y, Chopp M. Bone marrow stromal cells promote skilled motor recovery and enhance contralesional axonal connections after ischemic stroke in adult mice. Stroke. 2011; 42:740–744. [PubMed: 21307396]

Liu Z, Li Y, Zhang X, Savant-Bhonsale S, Chopp M. Contralesional axonal remodeling of the corticospinal system in adult rats following stroke and bone marrow stromal cell treatment. Stroke. 2008; 39:2571–2577. [PubMed: 18617661]

Lo EH. A new penumbra: Transitioning from injury into repair after stroke. Nat Med. 2008; 14:497–500. [PubMed: 18463660]

Lu YB, Iandiev I, Hollborn M, Korber N, Ulbricht E, Hirrlinger PG, Pannicke T, Wei EQ, Bringmann A, Wolburg H. Reactive glial cells: Increased stiffness correlates with increased intermediate filament expression. FASEB J. 2011; 25:624–631. others. [PubMed: 20974670]

Macauley SL, Pekny M, Sands MS. The role of attenuated astrocyte activation in infantile neuronal ceroid lipofuscinosis. J Neurosci. 2011; 31:15575–15585. [PubMed: 22031903]

Marin-Padilla M. Prenatal development of fibrous (white matter), protoplasmic (gray matter), and layer I astrocytes in the human cerebral cortex: A Golgi study. J Comp Neurol. 1995; 357:554–572. [PubMed: 7545703]

Mazzanti M, Sul JY, Haydon PG. Glutamate on demand: Astrocytes as a ready source. Neuroscientist. 2001; 7:396–405. [PubMed: 11597099]

McKeon RJ, Schreiber RC, Rudge JS, Silver J. Reduction of neurite outgrowth in a model of glial scarring following CNS injury is correlated with the expression of inhibitory molecules on reactive astrocytes. J Neurosci. 1991; 11:3398–3411. [PubMed: 1719160]

Menet V, Prieto M, Privat A, Gimenez y Ribotta M. Axonal plasticity and functional recovery after spinal cord injury in mice deficient in both glial fibrillary acidic protein and vimentin genes. Proc Natl Acad Sci U S A. 2003; 100:8999–9004. [PubMed: 12861073]

Morgenstern DA, Asher RA, Fawcett JW. Chondroitin sulphate proteoglycans in the CNS injury response. Prog Brain Res. 2002; 137:313–332. [PubMed: 12440375]

Morshead CM, Reynolds BA, Craig CG, McBurney MW, Staines WA, Morassutti D, Weiss S, van der Kooy D. Neural stem cells in the adult mammalian forebrain: A relatively quiescent subpopulation of subependymal cells. Neuron. 1994; 13:1071–1082. [PubMed: 7946346]

Nakagomi T, Taguchi A, Fujimori Y, Saino O, Nakano-Doi A, Kubo S, Gotoh A, Soma T, Yoshikawa H, Nishizaki T. Isolation and characterization of neural stem/progenitor cells from post-stroke cerebral cortex in mice. Eur J Neurosci. 2009; 29:1842–1852. others. [PubMed: 19473237]

Nakazawa T, Takeda M, Lewis GP, Cho KS, Jiao J, Wilhelmsson U, Fisher SK, Pekny M, Chen DF, Miller JW. Attenuated glial reactions and photoreceptor degeneration after retinal detachment in mice deficient in glial fibrillary acidic protein and vimentin. Invest Ophthalmol Vis Sci. 2007; 48:2760–2768. [PubMed: 17525210]

Nudo RJ. Mechanisms for recovery of motor function following cortical damage. Curr Opin Neurobiol. 2006; 16:638–644. [PubMed: 17084614]

Pallari HM, Eriksson JE. Intermediate filaments as signaling platforms. Sci STKE. 2006; 2006:pe53. [PubMed: 17179489]

Paxinos, G.; Franklin, K. The mouse brain in stereotaxic coordinates. San Diego: Academic Press; 1997.

Pekny M, Johansson CB, Eliasson C, Stakeberg J, Wallen A, Perlmann T, Lendahl U, Betsholtz C, Berthold CH, Frisen J. Abnormal reaction to central nervous system injury in mice lacking glial fibrillary acidic protein and vimentin. J Cell Biol. 1999; 145:503–514. [PubMed: 10225952]

Pekny M, Lane EB. Intermediate filaments and stress. Exp Cell Res. 2007; 313:2244–2254. [PubMed: 17524394]

Pekny M, Wilhelmsson U, Pekna M. The dual role of astrocyte activation and reactive gliosis. Neurosci Lett. 2014; 565:30–38. [PubMed: 24406153]

Potokar M, Kreft M, Li L, Daniel Andersson J, Pangrsic T, Chowdhury HH, Pekny M, Zorec R. Cytoskeleton and vesicle mobility in astrocytes. Traffic. 2007; 8:12–20. [PubMed: 17229312]

Potokar M, Stenovec M, Gabrijel M, Li L, Kreft M, Grilc S, Pekny M, Zorec R. Intermediate filaments attenuate stimulation-dependent mobility of endosomes/lysosomes in astrocytes. Glia. 2010; 58:1208–1219. [PubMed: 20544856]

Privat A. Astrocytes as support for axonal regeneration in the central nervous system of mammals. Glia. 2003; 43:91–93. [PubMed: 12761872]

Ransom BR, Ransom CB. Astrocytes: Multitalented stars of the central nervous system. Methods Mol Biol. 2012; 814:3–7. [PubMed: 22144296]

Reitmeir R, Kilic E, Reinboth BS, Guo Z, ElAli A, Zechariah A, Kilic U, Hermann DM. Vascular endothelial growth factor induces contralesional corticobulbar plasticity and functional neurological recovery in the ischemic brain. Acta Neuropathol. 2012; 123:273–284. [PubMed: 22109109]

Ridet JL, Malhotra SK, Privat A, Gage FH. Reactive astrocytes: Cellular and molecular cues to biological function. Trends Neurosci. 1997; 20:570–577. [PubMed: 9416670]

Rother J. Neuroprotection does not work. Stroke. 2008; 39:523–524. [PubMed: 18202309]

Schaar DG, Sieber BA, Dreyfus CF, Black IB. Regional and cell-specific expression of GDNF in rat brain. Exp Neurol. 1993; 124:368–371. [PubMed: 8287932]

Shannon C, Salter M, Fern R. GFP imaging of live astrocytes: Regional differences in the effects of ischaemia upon astrocytes. J Anat. 2007; 210:684–692. [PubMed: 17523937]

Silver J, Miller JH. Regeneration beyond the glial scar. Nat Rev Neuro-sci. 2004; 5:146–156.

Sofroniew MV. Reactive astrocytes in neural repair and protection. Neuroscientist. 2005; 11:400–407. [PubMed: 16151042]

Strens LH, Fogelson N, Shanahan P, Rothwell JC, Brown P. The ipsilateral human motor cortex can functionally compensate for acute contralateral motor cortex dysfunction. Curr Biol. 2003; 13:1201–1205. [PubMed: 12867030]

Swanson RA, Morton MT, Tsao-Wu G, Savalos RA, Davidson C, Sharp FR. A semiautomated method for measuring brain infarct volume. J Cereb Blood Flow Metab. 1990; 10:290–293. [PubMed: 1689322]

Trendelenburg G, Dirnagl U. Neuroprotective role of astrocytes in cerebral ischemia: Focus on ischemic preconditioning. Glia. 2005; 50:307–320. [PubMed: 15846804]

Vardjan N, Gabrijel M, Potokar M, Svajger U, Kreft M, Jeras M, de Pablo Y, Faiz M, Pekny M, Zorec R. IFN-gamma-induced increase in the mobility of MHC class II compartments in astrocytes depends on intermediate filaments. J Neuroinflammation. 2012; 9:144. [PubMed: 22734718]

Watson BD, Dietrich WD, Busto R, Wachtel MS, Ginsberg MD. Induction of reproducible brain infarction by photochemically initiated thrombosis. Ann Neurol. 1985; 17:497–504. [PubMed: 4004172]

Widestrand A, Faijerson J, Wilhelmsson U, Smith PL, Li L, Sihlbom C, Eriksson PS, Pekny M. Increased neurogenesis and astrogenesis from neural progenitor cells grafted in the hippocampus of GFAP$^{-/-}$Vim$^{-/-}$ mice. Stem Cells. 2007; 25:2619–2627. [PubMed: 17628017]

Wilhelmsson U, Bushong EA, Price DL, Smarr BL, Phung V, Terada M, Ellisman MH, Pekny M. Redefining the concept of reactive astrocytes as cells that remain within their unique domains upon reaction to injury. Proc Natl Acad Sci U S A. 2006; 103:17513–17518. [PubMed: 17090684]

Wilhelmsson U, Faiz M, de Pablo Y, Sjoqvist M, Andersson D, Widestrand A, Potokar M, Stenovec M, Smith PL, Shinjyo N. Astrocytes negatively regulate neurogenesis through the Jagged1-mediated Notch pathway. Stem Cells. 2012; 30:2320–2329. others. [PubMed: 22887872]

Wilhelmsson U, Li L, Pekna M, Berthold CH, Blom S, Eliasson C, Renner O, Bushong E, Ellisman M, Morgan TE. Absence of glial fibrillary acidic protein and vimentin prevents hypertrophy of astrocytic processes and improves post-traumatic regeneration. J Neurosci. 2004; 24:5016–5021. others. [PubMed: 15163694]

Zhao Y, Rempe DA. Targeting astrocytes for stroke therapy. Neurother-apeutics. 2010; 7:439–451.

Zuo J, Ferguson TA, Hernandez YJ, Stetler-Stevenson WG, Muir D. Neuronal matrix metalloproteinase-2 degrades and inactivates a neurite-inhibiting chondroitin sulfate proteoglycan. J Neurosci. 1998; 18:5203–5211. [PubMed: 9651203]

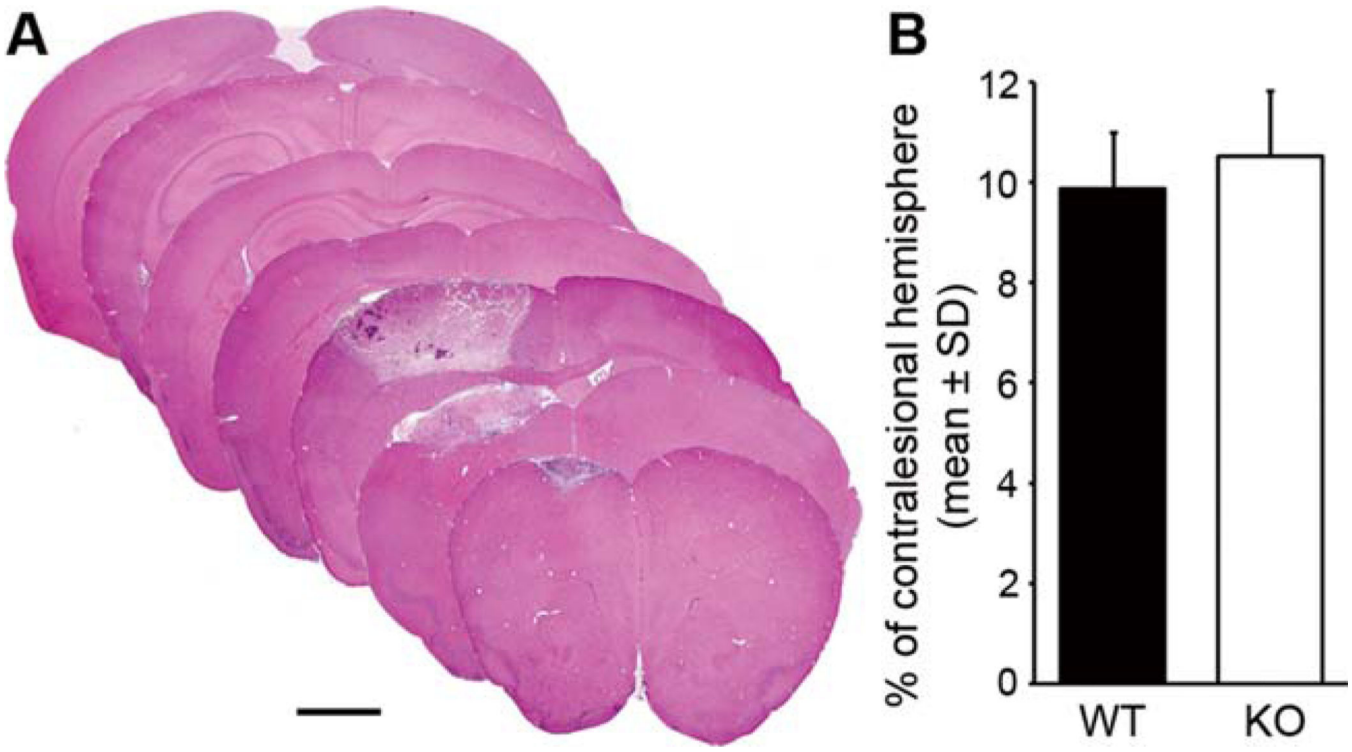

FIGURE 1.

Photothrombosis induced cortical ischemic infarct in mouse forelimb motor area by the Rose Bengal technique. A: A series of Hematoxylin and Eosin stained brain sections from a representative $GFAP^{-/-}Vim^{-/-}$ mouse show a typical photo-thrombotic lesion in the right sensorimotor cortex 28 days after ischemia. B: There was no significant difference in quantification of the stroke volume between the WT and knockout mice. Data are mean ± SD for $n = 10$ per group. Scale bar = 1 mm. [Color figure can be viewed in the online issue, which is available at wileyonlinelibrary.com.]

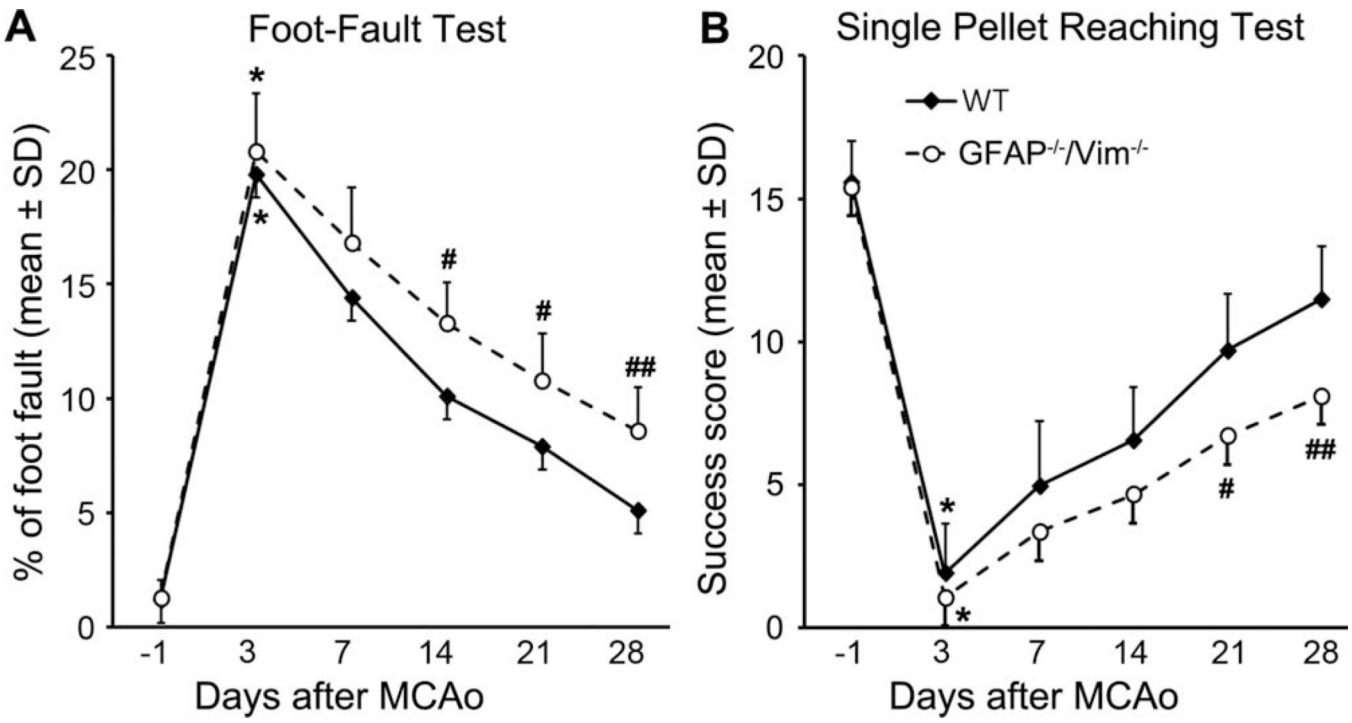

FIGURE 2.

Behavioral performance of the left forepaw. Mice were trained prior to stroke and baseline data were recorded. After photo-thrombosis of the right forelimb cortex, the left forepaw performance was significantly impaired in both foot-fault test (**A**) and single pellet reaching test (**B**; $n = 10$, $^{*}P<0.001$, day 3 vs. day −1). Both WT and GFAP$^{-/-}$Vim$^{-/-}$ mice exhibited gradual improvement, however, the recovery was significantly reduced in GFAP$^{-/-}$Vim$^{-/-}$ mice than in WT mice ($^{\#}P<0.05$, $^{\#\#}P<0.01$ vs. WT).

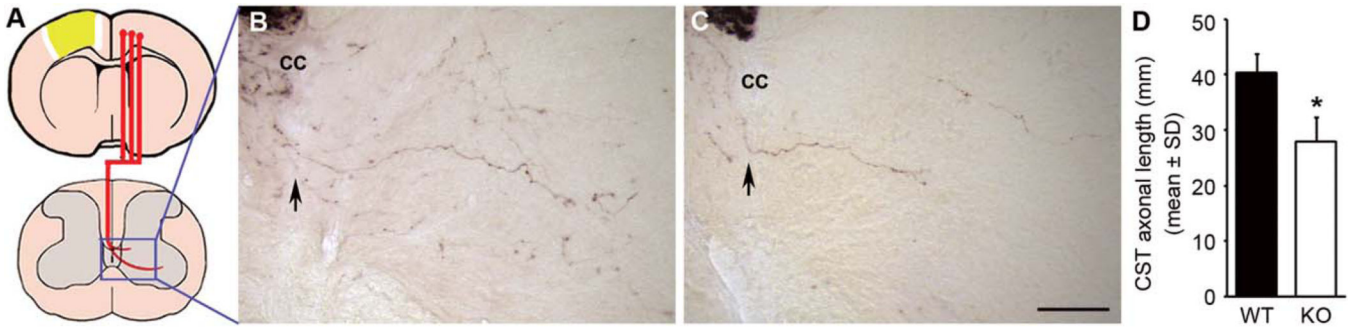

FIGURE 3.

Anterograde tracing of the CST originating from the contralesional cortex. **A**: A schematic drawing shows contralesional CST axonal labeling with BDA injected into the contralesional cortex and the location of pictures in B and C taken in the cervical spinal cord. **B** and **C**: Representative confocal pictures from WT and GFAP$^{-/-}$Vim$^{-/-}$ mice showing midline-crossing BDA-positive CST axons (*arrows*) sprouted into the denervated side of the ventral gray matter after stroke. **D**: Quantitative data showing that the BDA-labeled contralesional CST axonal length in the denervated side of the cervical cord was significantly reduced in mice lack GFAP and vimentin, compared with WT mice (n = 10/group, *P<0.001). CC stands for central canal indicating the midline of the spinal cord. Scale bar=100 μm. [Color figure can be viewed in the online issue, which is available at wileyonlinelibrary.com.]

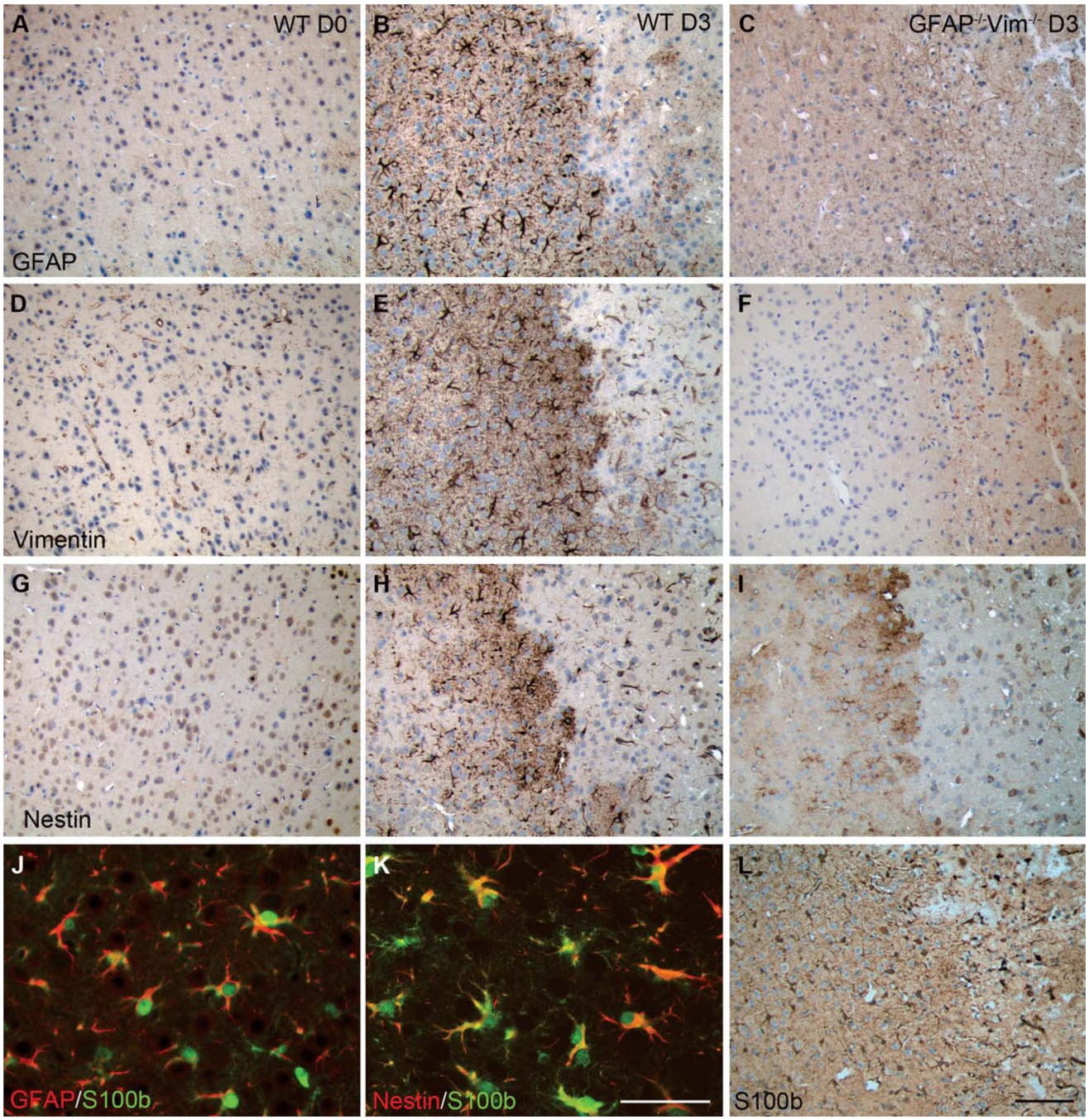

FIGURE 4.

Astrocytic activation was attenuated in the cortex after stroke. Immunostaining images show GFAP (**A–C**), Vimentin (**D–F**), and Nestin (**G–I**) in the cortex of adult normal WT mice (A, D, and G), day 3 stroke WT mice (B, E, and H), and $GFAP^{-/-}Vim^{-/-}$ mice (C, F, and I). Note that immunoreactivities of GFAP and Vimentin were increased in the cortical area around the lesion in WT mice and absent in $GFAP^{-/-}Vim^{-/-}$ mice, while immunoreactivity of Nestin was dramatically increased in WT mice and slightly increased in $GFAP^{-/-}Vim^{-/-}$ mice. Double immunostaining images show that S100β colocalized with GFAP (J) and

Nestin (K) in the WT mouse brain. In the $GFAP^{-/-}Vim^{-/-}$ mouse cortex, S100β-positive astrocytes were still present. Scale bar for A–I and L = 100 μm; for J and K550 μm.

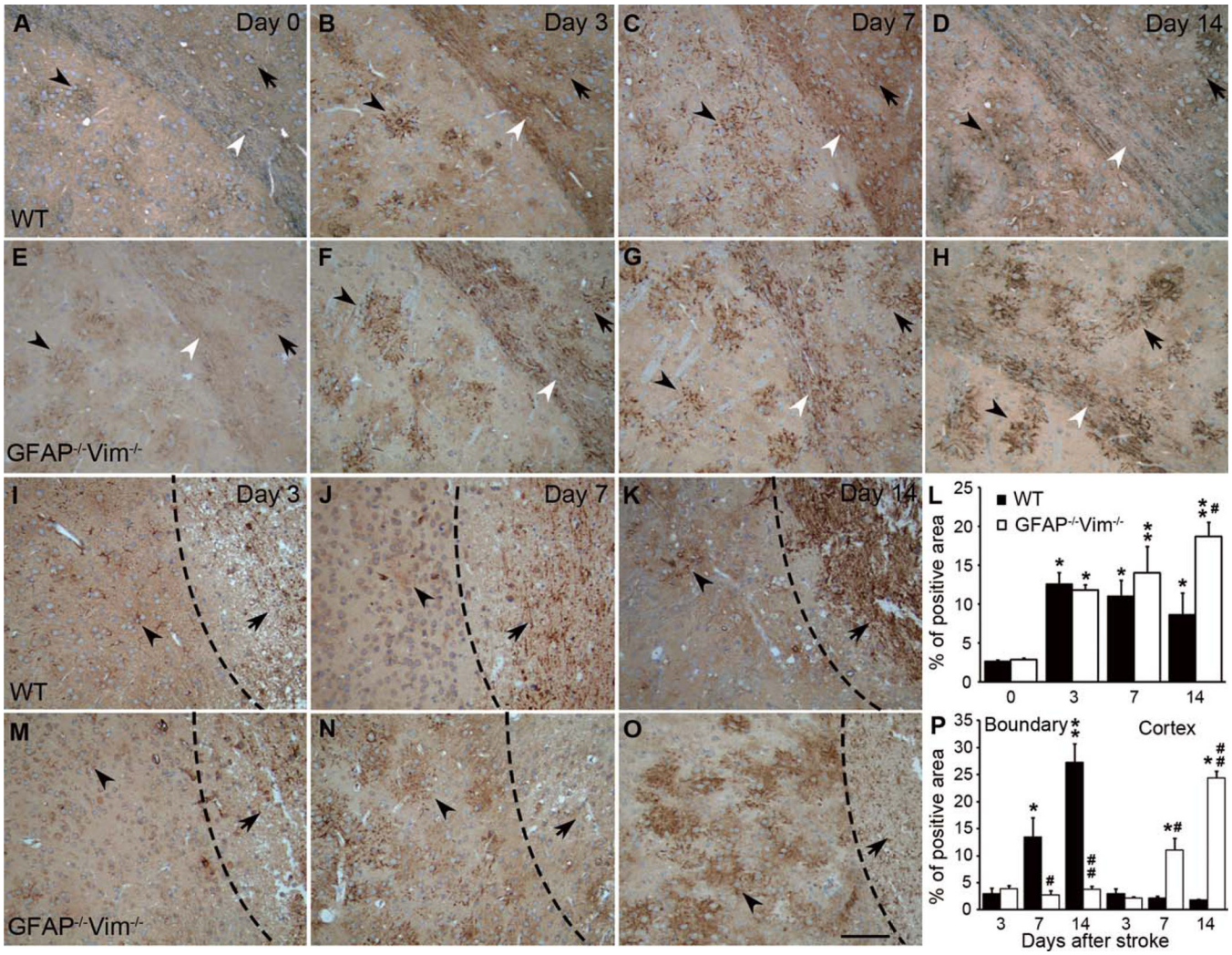

FIGURE 5.

CSPG immunoreactivity in the contralesional and ipsilesional cerebral hemispheres. In the contralesional hemisphere, increased positive staining areas were present in the cortex (*black arrows*), corpus callosum (*white arrowheads*), and striatum (*black arrowheads*) in the WT mice (**A–D**) and GFAP$^{-/-}$Vim$^{-/-}$ mice (**E–H**). In the ipsilesional hemisphere, increased positive staining areas were present in the lesion boundary zone in WT mice (arrows in **I–K**), but in the cortical area outer lesion boundary zone in GFAP$^{-/-}$Vim$^{-/-}$ mice (arrowheads in **M–O**). Quantitative data of positive area measurements indicate that CSPG expression was significantly increased in the contralesional hemisphere in both WT and GFAP$^{-/-}$Vim$^{-/-}$ mice (L, **P*<0.01, ***P*<0.0001 vs. normal control), and significantly higher expression was evident at day 14 after stroke in GFAP$^{-/-}$Vim$^{-/-}$ mice compared with WT mice ($^{\#}P$<0.01 vs. WT), while in the contralesional hemisphere, CSPG expression was significantly increased in the lesion boundary region in WT mice (P, **P*<0.01, ***P*<0.001 vs. normal control), and the cortical areas in GFAP$^{-/-}$Vim$^{-/-}$ mice (**P*<0.01, ***P*<0.001 vs. normal control), which was significantly different between WT and GFAP$^{-/-}$Vim$^{-/-}$ mice ($^{\#}P$<0.01, $^{\#\#}P$<0.001). *Dot lines* indicate the lesion border. Scale bar=100 μm.

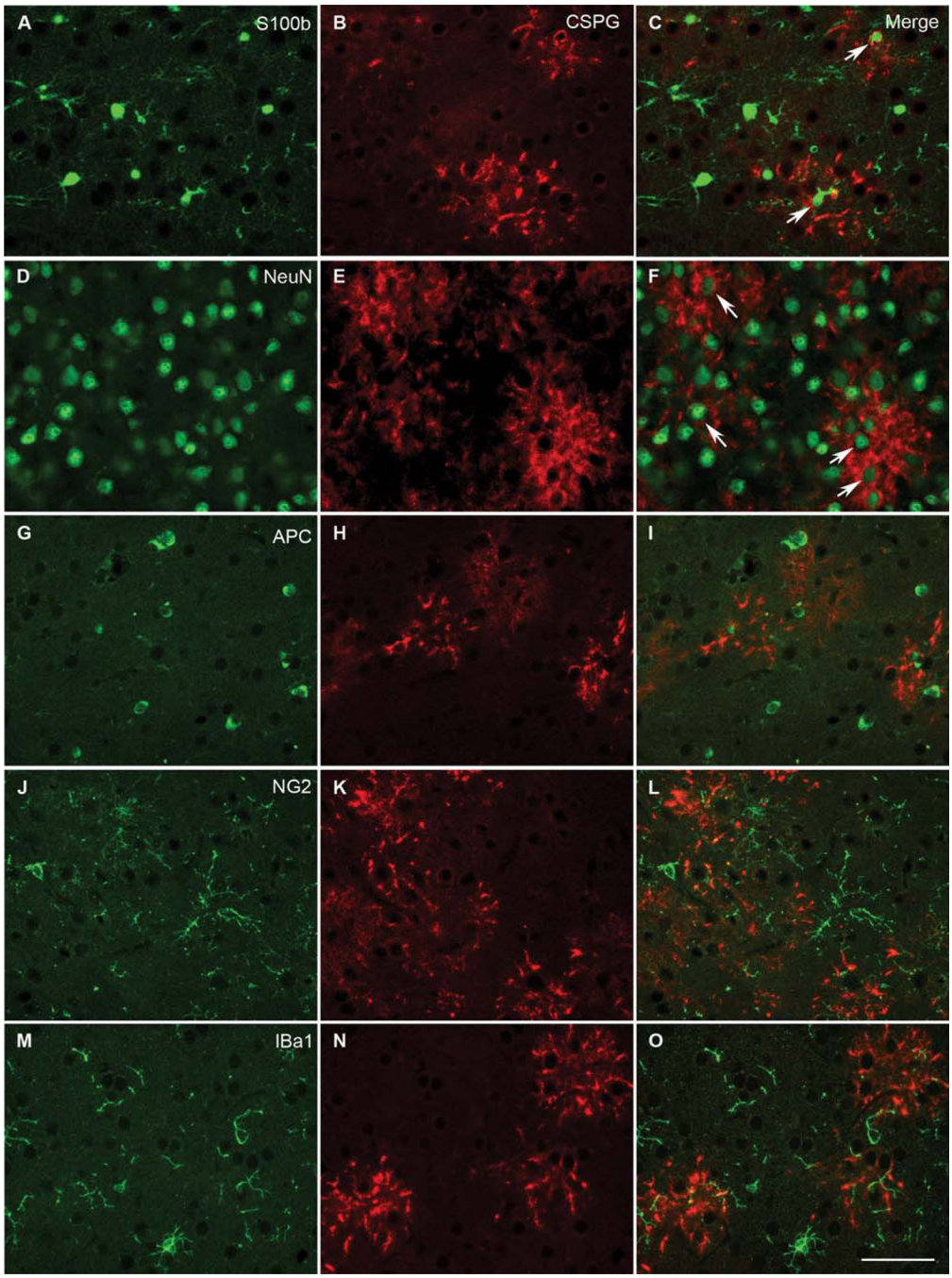

FIGURE 6.

Double immunostaining images show expression pattern of CSPG with S100β (an astrocytic marker; **A–C**), NeuN (a neuronal marker; **D–F**), APC (an oligodendrocytic marker; **G–I**), NG2 (a marker of oligodendrocyte precursor cells; **J–L**), and IBa1 (a microglial marker; **M–O**) in the $GFAP^{-/-}Vim^{-/-}$ mouse brains 7 days after stroke. Note that CSPG was present around a subpopulation of astrocytes (*arrows* in C) and neurons (*arrows* in D), but not

adjacent to oligodendrocytes, oligodendrocyte precursor cells, or microglia. Scale bar = 50 μm.